

RLinf: Flexible and Efficient Large-scale Reinforcement Learning via Macro-to-Micro Flow Transformation

Chao Yu¹², Yuanqing Wang³⁴, Zhen Guo³, Hao Lin³, Si Xu³, Hongzhi Zang¹, Quanlu Zhang³,
 Yongji Wu⁵, Chunyang Zhu³, Junhao Hu³, Zixiao Huang¹, Mingjie Wei², Yuqing Xie¹, Ke Yang²,
 Bo Dai⁶, Zhexuan Xu¹, Xiangyuan Wang⁴, Xu Fu³, Zhihao Liu², Kang Chen⁴², Weilin Liu³, Gang Liu¹,
 Boxun Li³, Jianlei Yang⁶, Zhi Yang⁴, Guohao Dai⁷³, Yu Wang^{1*}

¹Tsinghua University ²Zhongguancun Academy ³Infinigence AI

⁴Peking University ⁵UC Berkeley ⁶Beihang University ⁷Shanghai Jiaotong University

*Corresponding Author: yu-wang@tsinghua.edu.cn
 GitHub Repo: <https://github.com/RLinf/RLinf>

Abstract

Reinforcement learning (RL) has demonstrated immense potential in advancing artificial general intelligence, agentic intelligence, and embodied intelligence. However, the inherent heterogeneity and dynamicity of RL workflows often lead to low hardware utilization and slow training on existing systems. In this paper, we present RLinf, a high-performance RL training system based on our key observation that the major roadblock to efficient RL training lies in *system flexibility*. To maximize flexibility and efficiency, RLinf is built atop a novel RL system design paradigm called *macro-to-micro flow transformation* (M2Flow), which automatically breaks down high-level, easy-to-compose RL workflows at both the temporal and spatial dimensions, and recomposes them into optimized execution flows. Supported by RLinf worker’s adaptive communication capability, we devise *context switching* and *elastic pipelining* to realize M2Flow transformation, and a profiling-guided scheduling policy to generate optimal execution plans. Extensive evaluations on both reasoning RL and embodied RL tasks demonstrate that RLinf consistently outperforms state-of-the-art systems, achieving $1.1 \times \sim 2.13 \times$ speedup in end-to-end training throughput.

1 Introduction

The rapid progress of large language models (LLMs) has reached a point where further scaling model alone yields diminishing returns. To push intelligence beyond pretraining, reinforcement learning (RL) has emerged as a crucial paradigm. Recent advances such as RLHF [5, 29], GRPO [37], and RL for embodied agents [17, 18] and Deep Research [26, 50] all rely on RL to align LLMs with human preferences, improve reasoning, and enable autonomous interaction with complex environments. OpenAI and others predict that RL workloads will soon consume more computational resources than LLM pretraining [28], making RL training efficiency the most critical system concern.

However, efficient RL training for various scenarios such as reasoning, agentic and embodiment at the scale of modern

large models is challenging, which combines highly heterogeneous components with diverse workload characteristics and resource demands, such as LLM generation, inference and training, reward models, critic models, agent tooling and embodied environment simulators. For instance, LLM training consumes more accelerator (e.g., GPU) memory than LLM generation and inference (prefill-only generation) to maintain gradients and optimizer states, while LLM generation shows high dynamicity in response lengths, leading to low accelerator utilization. Moreover, components like LLM training support diverse parallelization strategies (e.g., data, tensor, pipeline parallelism), whereas others scale only via instance replication and may yield computation workloads distinct from common tensor computation in LLM, e.g., embodied simulators [7, 41] that require CPU for physics simulation and GPU graphics pipeline for 3D rendering.

Single execution mode of existing RL training systems fails to capture this diversity, leading to suboptimal efficiency. Collocated execution, where components sequentially occupy accelerators [39], suffers from the long-tail problem due to varying generation lengths, leaving accelerators idle. Disaggregated pipelining, where components run concurrently on separate accelerators with pipelining [10], mitigates the long-tail issue but introduces memory and computation imbalance (§2.2). Neither mode is universally optimal. Many RL workloads demand hybrid scheduling of the components to maximize efficiency, i.e., mixing collocation and pipelining in a more flexible way. However, supporting such flexible execution modes for a single programmed workflow is a significant challenge, as they often require different program structures and communication patterns. Also, identifying the right scheduling for a given workflow usually requires considerable manual tuning.

In this paper, we present RLinf, an RL training system that maximizes system flexibility to achieve efficient execution of a logically programmed RL workflow. At its core is a new paradigm called *macro-to-micro flow transformation* (M2Flow), i.e., macro logical flow with micro execution flow, which decouples the logical programming of RL workflows

from their physical execution planning. With M2Flow, developers program RL workflows imperatively, using a natural programming interface to define how components communicate and synchronize at a coarse granularity. RLinf then automatically transforms this logical flow into a fine-grained execution plan tailored to the workload and hardware at both spatial and temporal dimensions. By decoupling program semantics from execution modes, M2Flow lets developers preserve clean, intuitive workflows while the system explores a vast scheduling space, including temporal multiplexing, spatial pipelining, and hybrid scheduling.

RLinf achieves this through three key mechanisms. First, a *worker* abstraction that encapsulates each RL component for flexible placement, and built-in adaptive communication that allows direct and efficient communication between components regardless of worker and data placement. Second, elastic pipelining and automatic context switching that enable M2Flow transformation and expand the scheduling space, achieving pipeline granularity tuning and temporal accelerator multiplexing without modifying the logical workflow. Third, a profiling-guided scheduling policy that automatically selects efficient execution modes, balancing utilization across heterogeneous components. Together, these capabilities deliver both high flexibility, efficiency and programmability.

We implement RLinf using Ray for cluster management and worker process launch on remote nodes. Apart from the core mechanisms, RLinf also provides rich support for common RL components, algorithms, and models to facilitate RL workflow programming (§4). We extensively evaluate RLinf on both reasoning and embodied RL training across diverse models (e.g., Qwen2.5-1.5/7/32B [31], OpenVLA [17], OpenVLA-OFT [16]) and varying scales. Our evaluation shows that RLinf improves end-to-end throughput (i.e., tokens per second) by up to $1.5\times$ compared to state-of-the-art RL training systems in reasoning RL, and by up to $2.13\times$ in embodied RL. We have open-sourced the full codebase of RLinf to accelerate RL innovations in LLM era.

This paper makes the following contributions:

- Analysis of representative RL algorithms and scenarios, identifying characteristics of modern RL workflows and highlighting inefficiencies in current systems.
- A novel RL system paradigm M2Flow that decouples logical workflow programming from execution planning, enabling intuitive programming with flexible execution.
- A cohesive set of mechanisms, i.e., worker abstraction, elastic pipelining, context switching, adaptive communication, and a profiling-guided scheduler, that jointly realize M2Flow and enable efficient RL training.
- Comprehensive evaluations of RLinf across various RL workloads show that RLinf significantly improves efficiency and flexibility compared to existing approaches.

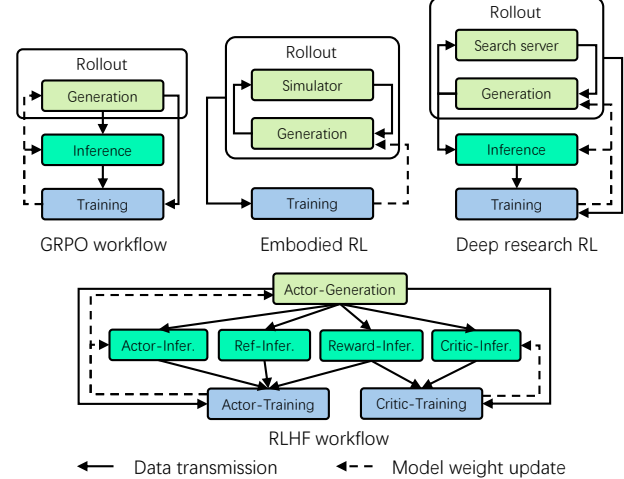


Figure 1: Diverse RL workflows in various scenarios.

2 Background and Motivation

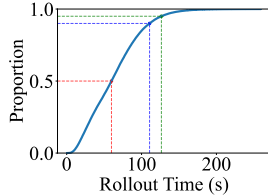
2.1 RL Workflows in LLM Era

Various RL Algorithms and Scenarios. With the slowdown of scaling gains in large language models, reinforcement learning has become increasingly important for advancing LLM intelligence. Unlike traditional RL, RL in the LLM era often involves multiple LLMs in the loop. Given the scale of modern models (tens to hundreds of billions of parameters), fitting RL training into available accelerators (e.g., GPUs) is already challenging. Figure 1 illustrates four representative RL workflows across different scenarios and algorithms.

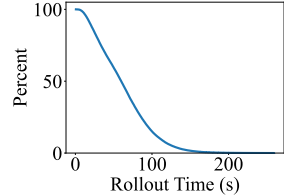
The simplest is GRPO [37], an RL algorithm designed to reduce reliance on reward models. It involves a single LLM that generates multiple responses, e.g., 8, for a query (i.e., Generation), computes logarithmic probabilities for these responses (i.e., Inference), and uses the results as training data to update the same model (i.e., Training). The updated weights are then synchronized back for inference and generation, completing one training iteration.

In contrast, the RLHF [29] workflow adopts PPO [36], resulting in a more complex design involving four LLMs. The actor model serves as the core policy, generating responses to queries. The reference model remains fixed to constrain the actor from drifting too far from its initialization. The reward model assigns scalar rewards to generated responses, while the critic model estimates expected rewards to stabilize training. Actor and critic are trainable, whereas reference and reward models are frozen. These components interact closely, as shown in the figure.

Beyond algorithms, RL workflows also vary by application scenario. In embodied intelligence [17, 18], RL relies on simulators that simulate the physical world. An LLM interacts with the simulator by generating actions and receiving



(a) CDF of response time.



(b) Unfinished responses.

Figure 2: The distribution of response lengths and the number of unfinished responses over time in the generation phase of a math RL experiment.

feedback, producing trajectories that serve as training data. Similarly, in Deep Research [26, 50], RL improves model performance through interaction with a search server that retrieves online information. The resulting rollout results are fed into training, while inference follows the GRPO-style workflow.

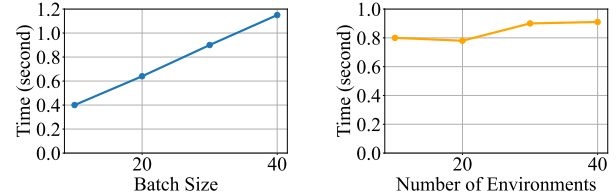
Characteristics of RL Workflows. RL workflows consist of heterogeneous components with distinct demands on GPU memory, computation cores, accelerator types, and parallelization strategies. For example, training requires substantially more GPU memory than inference to maintain gradients and optimizer states. Unlike training, generation often underutilizes GPU cores, as its matrix and vector multiplications are bottlenecked by memory bandwidth. Some components (e.g., simulator) run on CPUs, or use GPUs for non-tensor computations (e.g., 3D rendering). Parallelization also differs significantly, e.g., LLM training exploits data, tensor, and pipeline parallelism, whereas simulators typically scale only through multiple instances. Maximizing overall utilization across such heterogeneous components is a great challenge.

Further, RL workflows exhibit complex dependencies, primarily through data flow and weight updates. Data flow can occur at different granularity, e.g., per response between generation and inference, or at least a micro-batch of responses between generation and training. Some workflows even introduce cyclic data flows, such as in embodied RL and Deep Research (Figure 1), which further complicates coordination. Weight updates, in contrast, act as barriers that synchronize generation and training. These complex dependencies require more fine-grained scheduling.

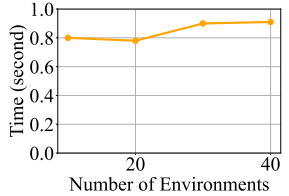
2.2 Inefficiencies in Diverse RL Workflows

We analyzed different RL workflows to identify the source of inefficiencies as follows.

Dynamism in Rollout Wastes Computation. The rollout phase is inherently dynamic. Lengths fluctuate across responses of the same query, and even more so across different queries. Embodied tasks such as grasping can take different



(a) Generation time.



(b) Simulator time.

Figure 3: The execution time of generation and simulator with different batch sizes respectively, batch size in simulator is the number of environments.

numbers of steps. In deep research, generating a report may involve varying numbers of search interactions. Since rollouts are executed in batches, these variations create a long-tail problem where a few slow queries block the entire phase from proceeding to inference or training. The problem commonly exists in the collocated mode (e.g., veRL [39]), where generation, inference, and training sequentially share GPUs by swapping between CPU and GPU memory. We conducted an experiment of a 7B math reasoning RL training [31] on 8 nodes with 8 H100 GPUs each, as shown in Figure 2. The number of unfinished responses quickly shrinks to less than 5%, where a very small set of long-tail responses stalls the generation, leaving many GPUs underutilized or idle. Scaling out with more GPUs worsens the problem as idle time grows.

Pipelining alleviates this by allocating fewer GPUs to generation and leaving the rest for inference and training. In this setup, inference and training start once partial samples are ready. However, pipelining introduces its own inefficiency since inference and training must wait for the first batch to be generated. Thus, neither approach is universally optimal, and supporting both collocated mode and pipelining within a single framework remains a significant challenge.

Simple Execution Modes Cannot Fit Diverse Components. Collocated and pipelined modes are two extremes, i.e., all components on the same GPUs versus fully disaggregated GPUs. Some RL workloads, however, do not fit neatly into either mode. Their diverse component characteristics require more flexible orchestration. Take embodied RL (Figure 1) as an example. Figure 3 shows computation profiles of generation and simulator. The execution time of simulator increases slightly with the number of environments and its GPU utilization remains low (i.e., <24%), while its memory usage grows linearly with the number of environments. In contrast, generation scales linearly in both runtime and memory with batch size, while keeping GPU cores highly utilized (i.e., >70%). Training consumes more memory, but its execution time is only one-third as long as generation's.

This profile rules out simple execution modes. The simulator should scale with as many parallel environments as

possible to reduce its total runtime. However, this prevents collocation with generation due to memory contention. A better choice is running on disaggregated GPUs with pipelining for higher efficiency. Training, in contrast, would waste compute if fully disaggregated, so it should share GPUs. After rollout, simulator and generation are swapped to CPU, and training takes over the GPU. The result is a hybrid mode that combines collocation and pipelining to balance efficiency.

Identifying Suitable Orchestration is Challenging. The orchestration of the hybrid mode depends on the analysis of the components. However, finding the most suitable orchestration for a given RL workflow is challenging, as the characteristics are diverse and the dependencies are complex. Manually enumerating options is tedious, time-consuming, and risks overlooking better choices. Moreover, no clear guidelines exist to identify the most suitable orchestration.

2.3 Flexibility as a Key to Efficiency

Maximizing computation efficiency for an RL workload requires flexible orchestration that aligns with component and workflow characteristics. However, adjusting the execution mode without changing the programmed workflow is challenging. Collocated and disaggregated pipelining modes differ significantly. Collocated mode operates at coarse-grained, phase-level execution. Each phase starts after the previous phase is complete. However, disaggregated pipelining runs at fine-grained, batch-level with precise timing to minimize pipeline bubbles. Mixing these modes further increases complexity. We advocate a system design that bridges this gap, enabling RL developers to maintain an intuitive, logically organized workflow while achieving high execution efficiency with flexible execution modes.

3 RLinf Design

3.1 Overview

In pursuit of efficient, flexible, and intuitive RL systems, we propose a new design paradigm termed M2Flow, i.e., *macro logical flow executed with micro execution flow*. In this paradigm, developers program the complex RL workflow by imperatively specifying the logical communication flow among the RL components at a coarse granularity (macro logical flow), while the system automatically transforms the workflow into a fine-grained execution flow (micro execution flow). Essentially, M2Flow decouples programmable code logic from the physical execution and scheduling of the individual RL components, so as to maximize the efficiency while minimizing the programming complexity.

Figure 4 shows the architecture of RLinf that realizes M2Flow. As illustrated, RLinf provides an easy-to-use procedural programming interface for users to construct RL workflows imperatively, which describe the data communication

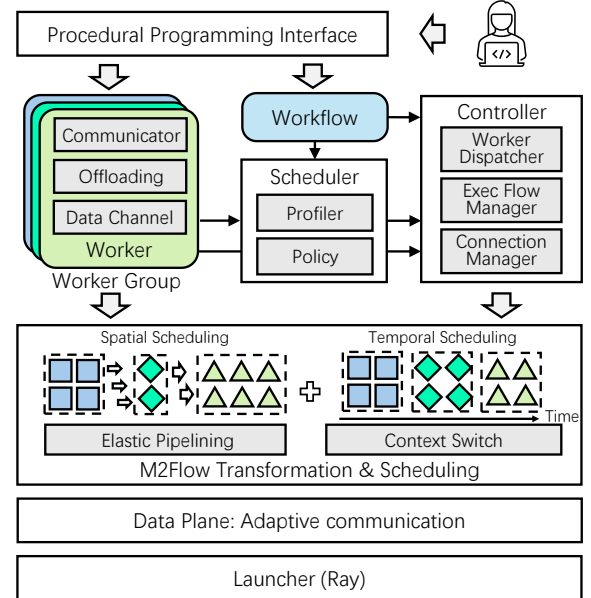


Figure 4: The architecture of RLinf.

and interaction among the RL components. RL components are then encapsulated as *workers* in RLinf, each implementing the main logic of this component. Workers are equipped with communication functionality to freely communicate with each other, as well as resource offloading mechanism to enable temporal multiplexing of hardware resources. This worker abstraction enables RLinf to retain substantial scheduling flexibility at both the spatial and temporal dimensions, while following the procedural workflow. Spatial scheduling assigns workers to accelerators, temporal scheduling determines their execution periods, and spatio-temporal scheduling governs their pipelined execution granularity.

To produce a desirable micro execution flow across these scheduling dimensions, the core of the scheduler module is a profiling-guided scheduling policy, which utilizes runtime profiling of worker characteristics to search for the optimal execution mode of each worker. Based on the determined execution mode, the Controller assigns workers to accelerators, manages inter-worker connections, and orchestrates the execution flow by dispatching function invocations to the corresponding workers. To realize this, two mechanisms named elastic pipelining and context switch are devised to enable spatial and temporal orchestration of workers, respectively. Adaptive communication utilities such as point-to-point communication and data channel act as the data plane to support scalable worker interactions. The entire system leverages Ray [24] to remotely launch and control workers.

3.2 Workflow Construction Interface

The design philosophy of RLinf is to maximize system flex-

```

class Worker:
    def send(self, obj, dst, async_op)
    def recv(self, src, async_op)
    @overload
    def onload(self)
    @overload
    def offload(self)

class RolloutWorker(Worker):
    def generate(self, in_channel, out_channel):
        with out_channel.device_lock:
            batch_size = 0
            while batch_size < self.total_batch_size:
                batch = in_channel.get()
                res = self.model.gen(batch)
                out_channel.put(res)
                batch_size += batch.size

```

(a) A typical RLinf worker.

```

class RLWorkflowRunner:
    def __init__(self):
        cluster = Cluster(num_nodes=4, devices_per_node=8)
        self.rollout_group = RolloutWorker.launch(cluster)
        self.actor_group = ActorWorker.launch(cluster)
        self.data_ch = Channel.create("Data")
        self.rollout_ch = Channel.create("Rollout")
    def run(self):
        for batch in batch_iterator:
            self._update_rollout_weights()
            self.data_ch.put(batch)
            self.rollout_group.generate(
                in_channel=self.data_ch,
                out_channel=self.rollout_ch
            )
        self.actor_group.train(self.rollout_ch).wait()

```

(b) A workflow runner example.

Figure 5: RLinf workflow programming interface.

ability to achieve high efficiency, which is also the guideline for RLinf’s programming interface design. To this end, unlike traditional graph-based declarative programming [1] that sacrifices control flow flexibility, debuggability and transparency for optimization opportunity, RLinf adopts a procedural programming paradigm that enables developers to flexibly express workflows imperatively. An example workflow based on this interface is shown in Figure 5. As shown, an RL program based on RLinf consists of two parts: (1) worker programs that define the logic of each RL component (e.g., simulator, LLM generation, actor training), and (2) a workflow runner that orchestrates the overall workflow by invoking the workers’ core functions and defining inter-worker interactions.

Figure 5a demonstrates a typical worker implementation atop RLinf. The base `Worker` class provides communication primitives such as `send` and `recv` for inter-worker communication. All workers inherit from the base class automatically gains the capability to communicate with other workers (§3.5), which is also the foundation for higher-level communication facilities like the data channel. To manage limited device resources like GPU memory, all workers are required to implement resource management functions (`onload` and `offload`) for acquiring and releasing the resources.

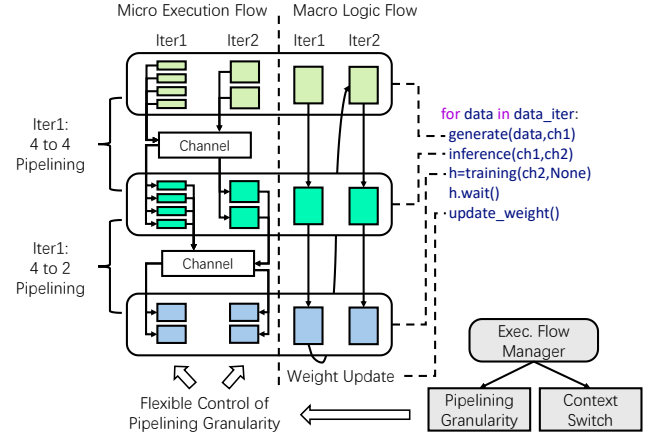


Figure 6: The M2Flow execution logic.

After implementing workers, developers can compose the overall RL workflow as in Figure 5b. First, the runner launches workers on a cluster of nodes and devices in an SPMD manner. The scheduler module decides the placement of each worker process before its launch, which can also be manually specified if desired. All processes of the same worker are collectively managed via the `WorkerGroup` abstraction of RLinf (e.g., `rollout_group`), which automatically assumes the public functions defined in the worker class and dispatches them to all (or a selective portion) of the worker processes if invoked. The functions of a `WorkerGroup` is inherently asynchronous and returns a result handle, whose `wait` primitive provides synchronization barriers, enabling the computations on certain granularity of data. For example, in GRPO training, rollout can proceed per query, but normalization must aggregate all responses for a query, which pauses the pipeline at this step until normalization completes. The core facility for connecting the data flow among distributed worker groups is the data channel (detailed in §3.5), which decouples the control and data flows of dependent components, enabling highly flexible programming while exposing a broad optimization space, as shown below.

3.3 M2Flow Transformation

The programming interface shown in Figure 5b offers a flow-like programming model, with which developers describe the high-level, logical control and data flows among workers. Having obtained the logical flows, RLinf follows the M2Flow paradigm to transform the logical flows (i.e., how should the workers run) into the concrete execution flow, i.e., where (spatial) and when (temporal) should the workers run. In this section, we focus on two enabling mechanisms of M2Flow transformation and flexible scheduling—elastic pipelining and context switching. In §3.4, we will describe the scheduling policy that determines the optimal execution flow.

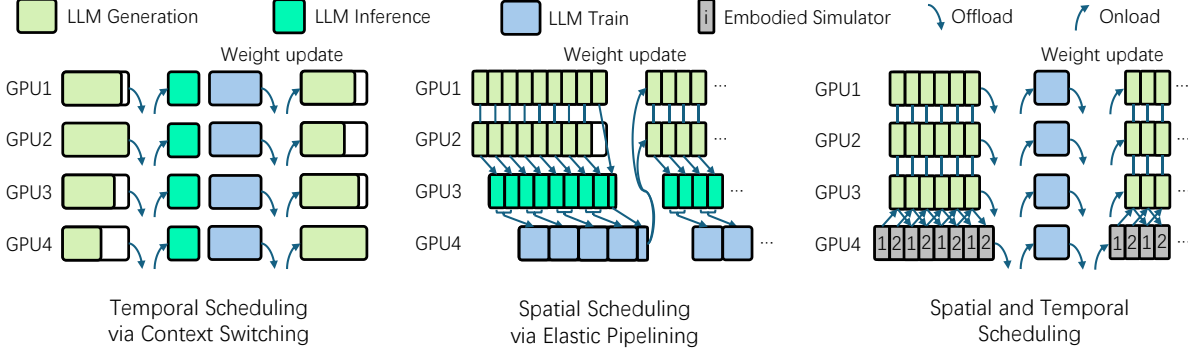


Figure 7: Spatial and temporal scheduling of workers.

Based on the programmed workflow, the key idea of M2Flow transformation is to control the spatial and temporal scheduling of workers by throttling their data processing granularity and concurrent resource accesses, respectively.

Spatial Scheduling via Elastic Pipelining. For spatial scheduling, workers can be executed in a pipelined manner with different number of accelerators/devices. To maximize pipeline flexibility, RLinf introduces elastic pipelining to enable workers to flexibly process data at different granularity with the given device resources. Elastic pipelining builds upon our insight that in RL training and agentic scenarios, most workers follow the SPMD pattern, allowing execution across varying batch sizes. For instance, LLM serving engines like SGLang and vLLM can process a single prompt or a list of prompts at a time, and inference (i.e., prefill-only computation of a model) similarly supports single-batch or multi-batch execution. This flexibility enables the Execution Flow Manager of RLinf to achieve flexible pipelining of a worker task via dynamic data granularity—output data can be forwarded once a configured size of data batch is ready, allowing downstream workers to start earlier with smaller batches or later with larger batches. Notably, the scheduling space is further affected by individual worker’s internal computation semantics. For example, training workers operate with both the micro-batch and global-batch concepts—the micro-batch defines forward/backward units, while the global-batch determines when model updates occur.

Temporal Scheduling via Automatic Context Switching. Beyond spatial scheduling, RLinf also supports natural temporal multiplexing of devices via automatic context switching, further expanding the scheduling space. Context switching enables workers that cannot co-reside in the same accelerators with limited device resources (e.g., GPU memory) to share devices by executing sequentially. In RLinf, this is realized via a distributed device lock of the data channel facility, i.e., `device_lock` as shown in Figure 5a. This lock serves as the primitive to throttle concurrent resource access by multiple workers on the same devices and have data flow dependencies,

i.e., producers and consumers of the same channel. Before using device resources, a worker must acquire the lock, whose state is globally consistent to all workers and can only be changed atomically, thus ensuring exclusive access to the resources. Upon lock acquiring, the worker’s device resources are automatically loaded by calling the `onload` function of the worker if the resources have been offloaded. After completing its task, the worker releases the lock and offloads its resources via the `offload` function to free up device resources for children workers in the workflow. Unlike conventional lock, the device lock leverages the data channel’s data dependency information to define lock acquiring priority, i.e., children workers that depend on the outputs of parent workers can only acquire the lock after the parents have enqueued data and released the lock, so as to avoid lock contention and deadlock. Also, it utilizes device placement information from the Controller to avoid unnecessary resource loading and offloading when workers are placed on different devices.

M2Flow Execution. Figure 6 shows how M2Flow manages execution. The workflow is written imperatively, i.e., a for loop iterating over main logic, with three workers, i.e., rollout, inference, and training. A rollout task such as `generate(data, ch1)` processes data and enqueues results to channel `ch1`. The Execution Flow Manager can divide the input data into smaller chunks, allowing workers to process outputs at a smaller data granularity. Alternatively, tasks can be coalesced into fewer, larger sub-tasks with larger data chunks to realize different temporal scheduling. Meanwhile, the device lock enables automatic resource management among workers with data dependencies, enabling spatial scheduling via context switching.

With M2Flow, user-defined workflows can be orchestrated across a complete spatial-temporal scheduling space. Figure 7 illustrates several representative execution modes suited to different RL workloads and configurations.

The left part of Figure 7 shows pure temporal scheduling, where each worker occupies all accelerators. Once a worker completes its task, it is swapped out and the next worker is swapped in. For the illustrated case, since inference and train-

Algorithm 1: Worker scheduling policy.

Input : Workflow graph G , number of devices N .
Output : A worker schedule S_{best} and its estimated time T_{best} .

```

1  $D_{table} \leftarrow \{\};$  // graph map to (time, schedule)
2  $G_{dag} \leftarrow \text{ConvertCircleToNode}(G);$ 
3  $T_{best}, S_{best} \leftarrow \text{FindSchedule}(G_{dag}, N, D_{table});$ 
4 Function  $\text{FindSchedule}(G, N, D_{table})$ :
5   if  $(G, N)$  in  $D_{table}$  then
6     | return  $D_{table}[(G, N)];$ 
7   end
8   if  $G$  is a node then
9     | return  $T_{perf}, S_{node};$ 
10  end
11   $T_{best} \leftarrow +\infty; S_{best} \leftarrow \text{None};$ 
12  for  $G_s, G_t$  in  $\text{TraverseStCuts}(G)$  do
13    /*  $G_s$  and  $G_t$  share the same gpus */
14     $T_s, S_s \leftarrow \text{FindSchedule}(G_s, N, D_{table});$ 
15     $T_t, S_t \leftarrow \text{FindSchedule}(G_t, N, D_{table});$ 
16     $D_{table}[(G_s, N)] \leftarrow (T_s, S_s);$ 
17     $D_{table}[(G_t, N)] \leftarrow (T_t, S_t);$ 
18    if  $T_{best} > T_s + T_t$  then
19      |  $T_{best} \leftarrow T_s + T_t; S_{best} \leftarrow \text{shared}(S_s, S_t);$ 
20    end
21    /*  $G_s$  and  $G_t$  use different devices */
22    for  $N_s, N_t$  in  $\text{TraverseGpuNum}(N)$  do
23      /*  $N_s + N_t$  equals  $N$  */
24       $T_s, S_s \leftarrow \text{FindSchedule}(G_s, N_s, D_{table});$ 
25       $T_t, S_t \leftarrow \text{FindSchedule}(G_t, N_t, D_{table});$ 
26       $D_{table}[(G_s, N_s)] \leftarrow (T_s, S_s);$ 
27       $D_{table}[(G_t, N_t)] \leftarrow (T_t, S_t);$ 
28      if  $T_{best} > \text{PipeliningTime}(T_s, T_t)$  then
29        |  $T_{best} \leftarrow \text{PipeliningTime}(T_s, T_t);$ 
30        |  $S_{best} \leftarrow \text{pipeline}(S_s, S_t);$ 
31      end
32    end
33  end
34  return  $T_{best}, S_{best};$ 
35 end

```

ing share the same model weights, no offloading or reloading is required. This mode is particularly useful when a worker must use all devices to be runnable, such as a large model’s training. However, it suffers from GPU idleness due to long-tail effects, e.g., the longest response length in the rollout stage determines the overall completion time of the stage.

The middle part illustrates spatial scheduling, where workers are assigned to separate GPUs. Because workers depend on one another, pipelining is applied to mitigate idle time. Achieving efficient pipelining requires balancing resources across workers so that their execution times align.

Finally, RL workflows are often too complex for purely temporal or spatial scheduling to remain efficient. M2Flow therefore supports hybrid scheduling, as shown on the right of Figure 7. Some workers are distributed across GPUs with pipelined execution, but once the workers’ stage completes, they can be swapped out and replaced by successors to continue the workflow.

3.4 Scheduling Policy

RLinf offers a large scheduling space through flexible orchestration of workers. Finding the most efficient execution mode for a given workflow is challenging. Thus, RLinf introduces two modules: the profiler and the scheduler. The profiler measures each component’s execution time and memory usage under different granularity, i.e., the execution batch sizes. These results are then fed to the scheduler, which searches the space and determines the final placement and execution plan. Specifically, the plan specifies GPU assignments, pipelining configurations and data processing granularity.

To determine the optimal worker scheduling, RLinf constructs a workflow graph in a just-in-time manner. The graph is extracted during profiling, when the workflow is executed, by tracing the data flow among workers through the communication primitives.

The scheduling algorithm, shown in Algorithm 1, recursively partitions the workflow graph into two subgraphs, G_s and G_t , connected by directed edges known as the *s-t cuts* [8]. For each partition, it evaluates the time cost of both the temporal and spatial scheduling policies. In the temporal scheduling, G_s and G_t share the same set of devices (e.g., GPUs)— G_s processes its batch, and upon completion G_t consumes its output. In the spatial scheduling, G_s and G_t are assigned to disjoint device sets and executed in a pipelined fashion. The scheduler uses the profiling results to find the optimal device allocation and data processing granularity for each subgraph. The algorithm then selects the most performant scheduling, and applies this process recursively until each subgraph reduces to a single node, at which point the node returns its profiled execution time under the assigned placement.

Modeling the execution time of G_s and G_t is the key to finding the optimal scheduling. In the temporal scheduling where workers share devices, the cost is the sum of G_s and G_t plus any resource offloading and reloading overhead. In the spatial scheduling, the runtime is estimated as

$$T_{critical} + (M/m - 1) \times T_{bottleneck},$$

where $T_{critical}$ is the pipeline warmup and cooldown time, $T_{bottleneck}$ is the runtime of the slowest subgraph, M is the total batch size, and m is the data processing granularity.

Before invoking FindSchedule , the workflow graph is pre-processed to collapse cycles into single nodes. When recursion reaches such a node, its computation is evenly partitioned across GPUs. This avoids exhaustive partition enumeration while still achieving near-optimal performance.

3.5 Adaptive Communication

To support flexible worker orchestration, RLinf’s communication layer needs to realize two key design goals. **(1) Flexible.** Any two workers should be able to communicate with each other, regardless of the worker placement and program logic.

(2) Adaptive. Communication primitives should be able to adapt to arbitrary data living in different devices (CPUs and GPUs across nodes), while achieving maximum throughput of the underlying communication links.

However, existing collective communication libraries for GPU and CPU data, e.g., NCCL [27], Gloo [30], and MPI [9], fail to meet our goals as they are mostly built for standard communication patterns across a fixed number of processes in traditional model training and serving scenarios. In contrast, RL components manifest considerable spatial and temporal dynamicity. Spatially, components can collocate on the same device, or being distributed across different devices. Temporally, components can be launched or terminated at arbitrary times. However, state-of-the-art libraries like NCCL does not support flexible rank scaling and efficient intra-device communications. Furthermore, the data communicated between components can be complex data structures beyond standard contiguous GPU/CPU data buffer, e.g., a composition of multiple data buffer with varying sizes. Efficient handling of such data dynamicity is also missing in existing libraries.

Communication Protocol and Primitives. To achieve the design goals, we devise worker and data placement-aware communication protocol and primitives, which enhances existing CPU/GPU communication libraries in terms of both flexibility and performance in the RL scenario.

At the protocol level, RLinf features transparent connection lifecycle management, which avoids manual connection management as in traditional communication libraries, and handles dynamic worker placement and scaling automatically. Specifically, upon launch, each worker’s placement, IP and port information will be registered into a global worker manager. Connections among workers are then established with the information lazily when workers invoke communication primitives to reduce connection overhead and enhance scalability. When a group of workers establish a connection, the connection metadata is maintained both locally by workers and globally by a connection manager. When a worker is terminated, the connection manager will notify all connected workers to teardown the connection and release resources.

At the primitive level, like existing libraries, RLinf offers both synchronous and asynchronous send and recv primitives for point-to-point communication, as well as collective communication primitives like broadcast. Differently, RLinf’s primitives automatically exploit the worker and data placement information of the communicating workers to select the most efficient communication backend, e.g., NCCL for GPU-GPU communication, zero-copy cudaIPC for intra-GPU communication, and Gloo for CPU communication. For data dynamicity, both the asynchronous and synchronous primitives support arbitrary Python objects as the communication payload, which are serialized and deserialized in a structure-aware manner, i.e., data buffers are extracted from the objects and communicated directly with

out serialization/deserialization overhead. Also, data structure information is piggybacked in the communication metadata to facilitate efficient deserialization at the receiver side.

Load-Balancing Data Channel. Atop the above communication primitives, we further build a high-level FIFO queue-like communication facility (termed *data channel*) for producer-consumer worker communication in the workflow. This enables decoupling of both the control and data flows of producer and consumer workers, which is essential for flexible pipelining. The data channel maintains its data queue in a special channel worker process, and can be accessed by any other worker processes by passing the channel handle. The channel supports both CPU and GPU data, and can be configured for offloading GPU data to CPU to reduce GPU memory consumption. Furthermore, the data channel is enhanced with load-balancing capability. Each item enqueued to the channel can be assigned a weight value, which is used to balance the load across multiple consumers dequeuing from the channel. The consumers can also define custom load-balancing policies, which are invoked by the channel upon each dequeue operation to select the desired items from the channel.

4 Implementation

RLinf is implemented in 20K lines of Python code. Among them, 5K lines are for the core worker, controller, and scheduler components. 2K for common workers such as rollout workers based on serving engines like SGLang, vLLM and HuggingFace Transformers, training actors based on Megatron and FSDP, and embodied simulators, which can be used out of the box for any future RL models and workflows. The remaining 13K lines are mostly rich supports for various RL algorithms like PPO and GRPO. Notably, a typical workflow runner like the LLM reasoning RL workflow implementation is less than 100 lines of code, and requires no code changes to be scheduled both temporally and spatially.

Currently, RLinf supports not only traditional LLM-based reasoning RL, but also agentic RL with tooling, and embodied RL involving complex workloads like 3D rendering, physics simulation, and robotic control. For RL algorithms, RLinf supports popular algorithms like PPO [36], GRPO [37], DAPO [45], and REINFORCE++ [11], as well as some of their off-policy asynchronous versions. For models, we have implemented support for language models like Qwen [31], multi-modal models like VLM [2], and embodied models like VLA [16, 17] and Pi0 [42]. The rich RL workflow, algorithm and model support not only accelerates the development of new RL workflows with RLinf, but also demonstrates its generality, versatility and extensibility in practice.

Cluster Management and Device Allocation. RLinf leverages Ray to realize cluster management, launching worker processes on remote nodes, and dispatching worker function executions. RLinf does not rely on Ray for device allocation

to workers, because Ray only supports rigid packed-style (i.e., consecutive devices) or spread-style (i.e., spread-across-node first) resource allocation [24], which are not flexible enough for today’s complex and dynamic RL workflows. Instead, RLinf offers a flexible device allocation strategy, which allows each worker process to be allocated with any device or devices of any node across the cluster, by simply specifying the target devices’ global IDs.

Failure Monitoring. The multi-component and distributed nature of RLinf makes it prone to various types of failures, such as worker process crashes, node failures, and network issues. RLinf implements failure monitoring of worker processes by wrapping public worker function (which can be launched remotely) with a failure handler, which catches not only standard Python exceptions, but also registers signal handlers to catch native failures like segmentation faults and terminations. Upon catching any failure, the failure handler reports the failure, and commit suicide immediately to reduce log contamination of the failure chain effects. Meanwhile, the Controller runs a failure monitor thread for each worker process, which periodically checks the liveness of the worker process via Ray. Upon detecting a failure of any worker process, the Controller quickly kills the whole system, so as to avoid triggering misleading timeout errors on other workers requiring the output of the failed worker.

Performance Profiling. Performance profiling support is not only crucial for developers to understand system bottlenecks, but also serves as the key to our scheduling policy. Thus, RLinf provides worker-group-level timer for every public function invoked remotely by the workflow runner. The timer automatically captures the execution time of a worker function, whose value can be retrieved via the asynchronous handle returned by the corresponding worker group function; the values of all processes in the worker group will be reduced to a single value via a specified reduction method (e.g., mean, max, min). Beyond this, developers can also create custom timers for more fine-grained profiling of any code region, and retrieve the timer values similarly.

5 Evaluation

We extensively evaluate RLinf on both reasoning and embodied RL training tasks. Specifically, we focus on the following aspects. **(1) End-to-end Performance.** We show that RLinf consistently outperforms state-of-the-art RL systems by $1.1 \times \sim 2.13 \times$ on a variety of reasoning and embodied models under different cluster scales. **(2) Performance Breakdown.** We analyze the time consumption of different components, e.g., training, generation, inference, and simulator to demonstrate the effectiveness of RLinf’s optimizations. **(3) Model Performance.** We evaluate the models trained with RLinf on various benchmarks to demonstrate that RLinf can effectively improve model performance.

5.1 Experimental Setup

Models. We evaluate RLinf on two types of modern model families listed in [Table 1](#). For reasoning LLMs, we choose Qwen2.5 Models [31] distilled by DeepSeek-R1 with sizes ranging from 1.5B to 32B, which are widely used in the research community. For embodied models, we choose OpenVLA [17] and OpenVLA-OFT [16] models, both supervised-finetuned by RL4VLA [21] and SimpleVLA-RL [18]. OpenVLA and OpenVLA-OFT are two models widely applied by embodiment research community.

Table 1: Experiments setting.

Model	Environment	Type	Task	Baseline
Qwen2.5-1.5B	-	LLM	Text Generation	veRL
Qwen2.5-7B	-	LLM	Text Generation	veRL
Qwen2.5-32B	-	LLM	Text Generation	veRL
OpenVLA	ManiSkill	VLA	Embody	RL4VLA
OpenVLA-OFT	LIBERO	VLA	Embody	SimpleVLA-RL

Datasets and Environments. For reasoning LLMs, we use the AReal-boba-Data dataset [43]. This dataset integrates multiple standard datasets including DeepScaleR, Open-Reasoner-Zero, Light-R1, DAPO, NuminaMath (AoPS/Olympiad subsets), and ZebraLogic. Overly simple problems are filtered out to ensure dataset quality and effectiveness.

For VLAs, we employ two training environments: the LIBERO [20] benchmark and a pick-and-place task formulated in RL4VLA [21], which is implemented on the ManiSkill [41] framework. We refer to the latter as *ManiSkill* for brevity in the following sections.

Configuration. The model and environment configurations for LLM and embodied model experiments are detailed in [Table 2](#) and [Table 3](#), respectively. These settings remain consistent when scaling to a larger number of GPUs.

Table 2: Experiments setting of reasoning RL

Model Size	1.5B	7B	32B
Rollout Batch Size	512	512	512
Group Size	16	32	32
Sequence Length	28672	28672	28672
Actor TP Size	2	4	8
Rollout TP Size	1	2	4

Table 3: Experiments setting of embodied RL

Environment	ManiSkill	LIBERO
Number of Environments	256	512
Step	80	64

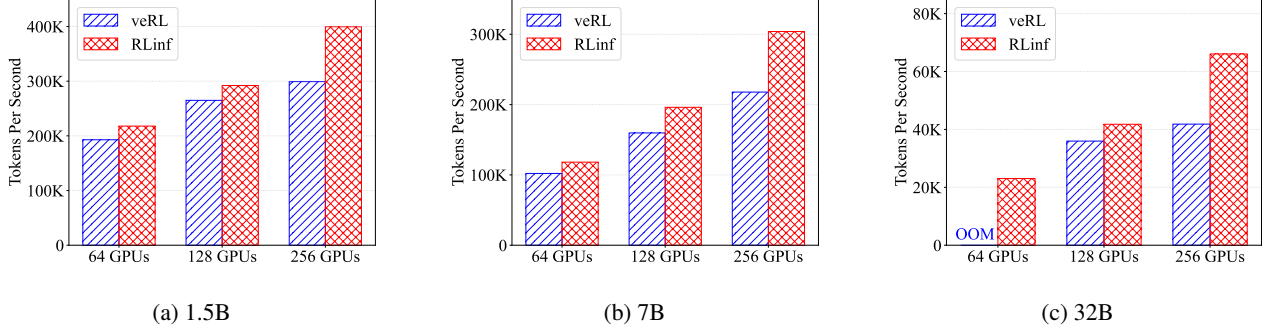


Figure 8: End-to-end throughput of RLinf and veRL under different cluster scale and model size settings.

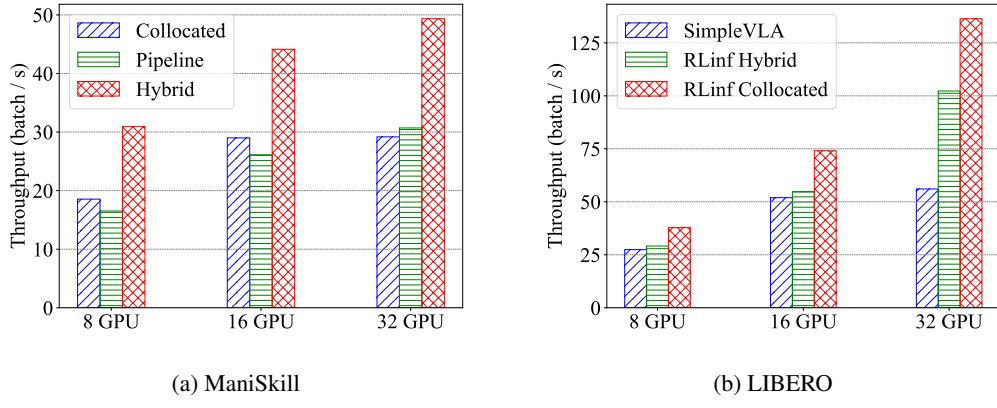


Figure 9: End-to-end throughput of RLinf and baselines under different cluster scale and placement strategy.

Testbed. We deploy RLinf on a H100 cluster with 32 nodes and 256 GPUs. Each node has 8 NVIDIA H100-80GB GPUs, and 2 Intel Xeon Platinum 8558@2.1 GHz CPUs with 48 core and 2TB memory. Intra-node communication utilizes NVLink, while inter-node communication uses 8 Mellanox ConnectX-7 RDMA NiCs per node, each provides 400 Gbps bandwidth with RoCEv2.

Baselines. For LLMs, we compare RLinf against veRL [39] v0.5, the state-of-the-art open-source RLHF system. We choose SGLang [49] as its rollout engine and Megatron-LM [40] as its training backend.

For embodied AI models, we compare RLinf against SimpleVLA-RL [18] and RL4VLA [21]. SimpleVLA-RL is built upon the veRL framework. It extends veRL with parallel multi-environment rendering for faster sampling, and adapt it into an integrated training–inference–rendering framework. RL4VLA is a recipe for efficient PPO training on VLAs, we integrated its core algorithm into RLinf and applied key optimizations. This ensures a fair and efficient comparison.

Metrics. For the LLM end-to-end experiment, we use RLHF throughput (tokens/sec) as the performance metric following [39], which is defined as dividing the total number of tokens in prompts and responses in a global batch by one

RLHF iteration time. For the embodied models, we use batch throughput (batches/sec), computed by dividing the number of batches by iteration time in one step. All reported performance numbers are averaged over 10 training iterations after warm-up.

RL Algorithms. For reasoning RL, we use the popular GRPO algorithm with following modifications:

- **Token-Level Loss:** Instead of averaging loss over the entire response sequence, we compute the average over tokens, as in DAPO. This prevents excessively long responses from dominating training and reduces their gradient impact.
- **Minibatch Early-Stop:** We discard minibatches with too large importance ratio to stabilize training.

We use a rule-based reward function, which will return 5 if the final boxed/numeric answer is correct else -5.

For embodied models, we use both PPO and GRPO for ManiSkill+OpenVLA and Libero+OpenVLA-OFT.

5.2 End-to-End Performance

Reasoning RL Training. Our evaluation demonstrates that RLinf consistently outperforms baseline systems across all

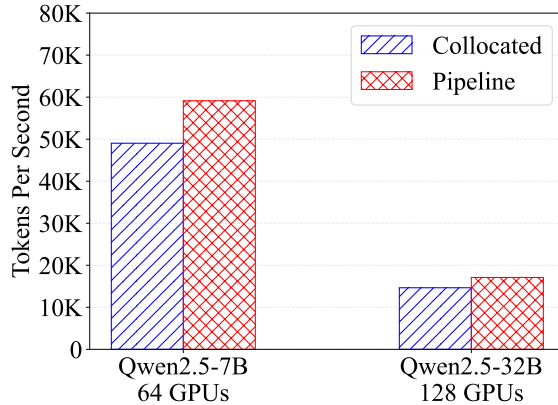


Figure 10: Throughput of RLinf under different placement modes and model size settings.

model scales. As shown in Figures 8a, 8b, and 8c, which present RLHF throughput results for GRPO on Qwen2.5 models at 1.5B, 7B, and 32B parameters, RLinf achieves a speedup ranging from $1.10\times$ to $1.58\times$ compared to veRL.

Moreover, Figure 8 reveals that veRL exhibits suboptimal performance scaling in multi-GPU environments. This limitation is primarily attributed to two factors: (1) its log probability computation becomes a computational bottleneck, as will be discussed in detail in Section 5.3; (2) the unoptimized rollout engine results in excessive peak GPU memory usage, necessitating a reduction in the memory allocated for the rollout engine’s KV cache. This constraint further diminishes its scalability.

As previously noted in Section 2.2, the dynamic and long-tailed nature of response generation results in GPU underutilization, a problem that becomes more pronounced in long-context RL training. Figure 10 compares performance between collocated and disaggregated modes under a context length of 28,672 and group size 8. The disaggregated mode yields a speedup of $1.17\times$ to $1.21\times$ over the collocated mode.

Embodied RL Training. Figure 9 presents the end-to-end throughput of RLinf and baseline methods in embodied AI training under different cluster sizes and placement strategies, with ManiSkill running on GPU and LIBERO on CPU.

For ManiSkill, RL4VLA is integrated under a disaggregated mode configuration. As shown in Figure 9a, RLinf achieves a $1.88\times$ speedup in hybrid mode on 8 GPUs. When scaling to 16 and 32 GPUs, overhead from model loading/of-flooding and state switching increases; however, the hybrid mode mitigates this cost through pipelined execution that overlaps computation and communication, still delivering a $1.61\times$ to $1.69\times$ speedup.

Although the hybrid mode yields significant improvements in ManiSkill, Figure 9b shows that the collocated mode performs better in LIBERO, achieving a $1.25\times$ to $2.13\times$ speedup.

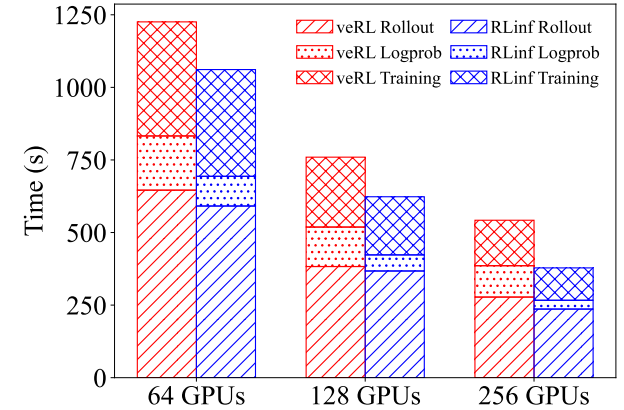


Figure 11: Latency breakdown of Qwen2.5 7B model training in Figure 8b.

Since LIBERO is a CPU-bound task, the training process is bottlenecked by CPU-based rollout. The collocated mode allocates all resources to the rollout stage, resulting in higher performance in this scenario.

5.3 Performance Breakdown

Figure 11 illustrates the latency breakdown for training the Qwen2.5-7B model, corresponding to the setup in Figure 8b. The performance of veRL is constrained by two main factors: first, its unoptimized rollout engine requires a reduction in KV cache memory allocation, which prolongs the rollout process; second, veRL exhibits longer inference times, further reducing its overall throughput.

Figure 12 presents a latency breakdown and comparison between collocated and disaggregated modes for the 7B model, complementing the results in Figure 10. It can be observed that despite allocating only 40 out of 64 GPUs to the rollout stage in disaggregated mode, the end-to-end rollout time increases by merely 14%. Moreover, both the inference and training stages—once their rollout results are ready—can execute concurrently with the rollout of other requests. This parallelization leads to a reduction in end-to-end iteration time and higher overall throughput.

Figure 13 presents a detailed performance breakdown of LIBERO, complementing the results shown in Figure 9b. RLinf demonstrates superior training efficiency in both hybrid and collocated modes. The improved rollout performance can be attributed to two key optimizations: (1) the elimination of redundant environment initialization during the rollout stage, and (2) the use of a single forward pass to compute both action and log probability, achieved with a modest increase in memory usage.

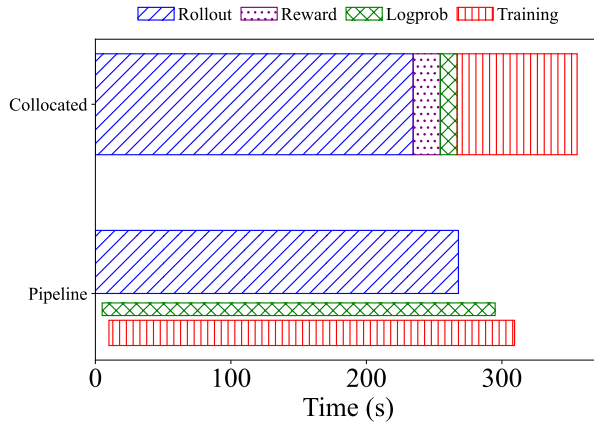


Figure 12: Latency breakdown and comparison for collocated and disaggregated modes on the 7B model in Figure 10. The width of bar is proportional to the number of GPUs. Note that under the disaggregated mode, the reward computation time is included within the rollout phase and is therefore not shown separately.

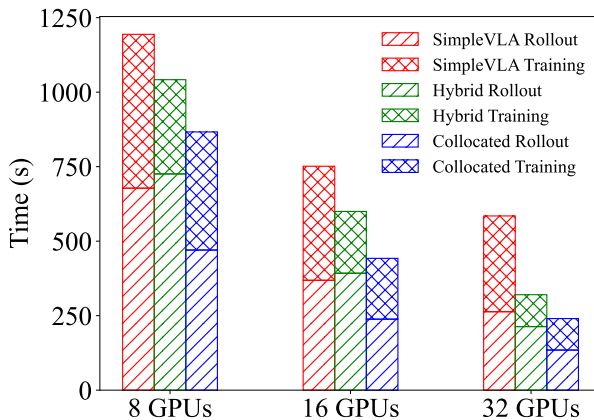


Figure 13: Latency breakdown of LIBERO in Figure 9b.

5.4 Algorithm Performance

We conducted comprehensive evaluation across various benchmarks for different modalities. Our benchmarks primarily consist of the following two categories:

- **Math Benchmark:** AIME 24, AIME 25, GPQA-diamond.
- **Embody Benchmark:** LIBERO, as well as custom pick-and-place tasks on ManiSkill with out-of-distribution (OOD) vision, semantic, and position challenges.

Reasoning RL Training. Using RLinf, we applied reinforcement learning to both DeepSeek-R1-Distill-Qwen-1.5B and DeepSeek-R1-Distill-Qwen-7B, presenting two new models: RLinf-math-1.5B and RLinf-math-7B. These models achieve best performance across multiple benchmarks among models of comparable scale, as shown in Table 4. RLinf-math-

1.5B outperforms all baseline models across all benchmarks, improving by up to 20 points over its base model, DeepSeek-R1-Distill-Qwen-1.5B. RLinf-math-7B achieves the highest performance on GPQA-diamond and leads in average benchmark scores among all compared models.

Embodied RL Training. To achieve reasonable reinforcement learning results in an embodied setting, the base models must exhibit a non-zero success rate. Therefore, we selected different base models for different environments and model types, each of which was initialized from a supervised fine-tuned OpenVLA or OpenVLA-OFT model. The detailed mapping between the final RL models and their base models is provided in Table 5. Note that the RL models are named according to the convention: RLinf-[model type]-[RL algorithm]-[environment].

Table 6 and Table 7 present the evaluation results of our trained models on the ManiSkill and LIBERO benchmarks, respectively. In the ManiSkill environment, the trained models demonstrate strong generalizability under out-of-distribution settings and achieve higher success rates than the baseline RL4VLA [21] checkpoint. On the LIBERO benchmark, our RL models exhibit significant performance improvement, attaining state-of-the-art success rates on all spatial, object, goal, and long tasks.

6 Related Works

RL Training Frameworks. RL training frameworks adopt varying system designs to support large-scale alignment tasks [5, 29], typically falling into either task-colocated or task-separated execution modes. For task-colocated systems, DeepSpeed Chat [44] and VERL [39] put all training phases on shared GPUs for simplified orchestration. In contrast, task-separated systems like NeMo-Aligner [38] and Open-RLHF [12] divide components across devices to improve modularity and scalability. AReal [10] further introduces asynchronous model updates algorithm upon task-separated systems to increase training throughput. RLinf differs from these frameworks by supporting dynamic transitions between colocated and separated execution modes based on runtime workload patterns.

Distributed Training Systems for LLM. A variety of distributed training frameworks have been developed to support large language models (LLMs) [19, 47, 48], alongside numerous system-level optimizations targeting memory usage [4, 13, 23] and communication efficiency [3, 15, 22]. Megatron-LM [40] adopts hybrid parallelism by combining tensor, pipeline, and data parallelism, significantly enhancing scalability for multi-billion parameter models. DeepSpeed [34] introduces the ZeRO series of optimizations [32, 33, 35], which partition optimizer states, gradients, and activations across devices, drastically reducing per-GPU memory requirements.

Table 4: Evaluation scores of RLinf-math-1.5B/7B and open-source models.

Model	AIME 24	AIME 25	GPQA-diamond	Average
1.5B models				
DeepSeek-R1-Distill-Qwen-1.5B (base model)	28.33	24.90	27.45	26.89
DeepMath-1.5B	37.80	30.42	32.11	33.44
DeepScaleR-1.5B-Preview	40.41	30.93	27.54	32.96
AReAL-1.5B-Preview-Stage-3	40.73	31.56	28.10	33.46
AReAL-1.5B-retrain*	44.42	34.27	33.81	37.50
FastCuRL-1.5B-V3	43.65	32.49	35.00	37.05
RLinf-math-1.5B	48.44	35.63	38.46	40.84
7B models				
DeepSeek-R1-Distill-Qwen-7B (base model)	54.90	40.20	45.48	46.86
AReAL-boba-RL-7B	61.66	49.38	46.93	52.66
Skywork-OR1-7B	66.87	52.49	44.43	54.60
Polaris-7B-Preview	68.55	51.24	43.88	54.56
AceMath-RL-Nemotron-7B	67.30	55.00	45.57	55.96
RLinf-math-7B	68.33	52.19	48.18	56.23

Table 5: Base Model Mapping For Embodiment RL Models

Model Name	Base Model
RLinf-OpenVLA-GRPO-ManiSkill3-25ood	gen-robot/openvla-7b-rlvla-warmup
RLinf-OpenVLA-PPO-ManiSkill3-25ood	
RLinf-OpenVLAOFT-GRPO-ManiSkill3-25ood	RLinf/Openvla-oft-SFT-libero10-trajall
RLinf-OpenVLAOFT-PPO-ManiSkill3-25ood	and RLinf/RLinf-OpenVLAOFT-ManiSkill-Base-Lora
RLinf-OpenVLAOFT-GRPO-LIBERO-spatial	Haozhan72/Openvla-oft-SFT-libero-spatial-traj1
RLinf-OpenVLAOFT-GRPO-LIBERO-object	Haozhan72/Openvla-oft-SFT-libero-object-traj1
RLinf-OpenVLAOFT-GRPO-LIBERO-goal	Haozhan72/Openvla-oft-SFT-libero-goal-traj1
RLinf-OpenVLAOFT-GRPO-LIBERO-long	Haozhan72/Openvla-oft-SFT-libero-long-traj1

Table 6: OpenVLA and OpenVLA-OFT models success rate results on ManiSkill3

Model	Algorithm	Vision	Semantic	Position	Average
gen-robot/openvla-7b-rlvla-rl	PPO	76.6%	75.4%	77.6%	76.1%
RLinf-OpenVLAOFT-GRPO-ManiSkill3-25ood	GRPO	84.6%	51.6%	42.9%	61.5%
RLinf-OpenVLAOFT-PPO-ManiSkill3-25ood	PPO	80.5%	56.6%	56.1%	64.5%
RLinf-OpenVLA-GRPO-ManiSkill3-25ood	GRPO	74.7%	74.4%	81.6%	75.5%
RLinf-OpenVLA-PPO-ManiSkill3-25ood	PPO	82.0%	80.6%	89.3%	82.2%

Table 7: OpenVLA-OFT model results on LIBERO

Model	LIBERO				
	Spatial	Object	Goal	Long	Avg.
Octo	78.9	85.7	84.6	51.1	75.1
OpenVLA	84.7	88.4	79.2	53.7	76.5
Nora	92.2	95.4	89.4	74.6	87.9
π_0 +FAST	96.4	96.8	88.6	60.2	85.5
π_0	96.8	98.8	95.8	85.2	94.2
UniVLA	96.5	96.8	95.6	92.0	95.2
OpenVLA-OFT One-Trajectory SFT					
Baseline	56.5	25.6	45.6	9.7	34.4
RLinf	99.0	99.0	99.0	94.4	97.9
Δ	+42.5	+73.4	+53.4	+84.7	+63.5

Distributed reinforcement learning systems share similar challenges with LLM training frameworks in scaling large models across multiple devices under resource constraints. However, RL workflows are inherently more dynamic due to interactive data generation and asynchronous updates, making system-level optimization more complex and challenging.

Dataflow System. Traditional dataflow systems [6, 14, 25, 46] have played a foundational role in scaling large-scale data processing and machine learning workloads. These systems rely on static task graphs and centralized scheduling, making them highly efficient for batch or streaming jobs with predictable structures. In contrast, reinforcement learning training pipelines typically involve dynamic task graphs with asynchronous components such as data collection, policy updates, and training. These workloads demand greater flexibility in scheduling and coordination than traditional systems provide. Modern frameworks like Ray [24] address this gap with actor-based execution and decentralized control, making them well-suited for orchestrating complex RL workflows.

7 Conclusion

Reinforcement learning is poised to surpass pretraining as the driving force behind LLM progress, but its workflows are too diverse and dynamic for rigid execution models. RLinf shows that by decoupling workflow logic from execution through the novel macro-to-micro transformation mechanism, we can unlock both efficiency and programmability. Beyond RL, we see this approach as a blueprint for future AI runtimes: systems that flexibly orchestrate heterogeneous components, e.g., training, inference, simulation, and reasoning, under one unified execution framework. We believe RLinf marks an early step toward the operating system for AI workloads.

References

[1] Martín Abadi, Paul Barham, Jianmin Chen, Zhifeng Chen, Andy Davis, Jeffrey Dean, Matthieu Devin, San-

jay Ghemawat, Geoffrey Irving, Michael Isard, et al. Tensorflow: a system for large-scale machine learning. In *12th USENIX symposium on operating systems design and implementation (OSDI 16)*, pages 265–283, 2016.

[2] Shuai Bai, Keqin Chen, Xuejing Liu, Jialin Wang, Wenbin Ge, Sibo Song, Kai Dang, Peng Wang, Shijie Wang, Jun Tang, et al. Qwen2. 5-vl technical report. *arXiv preprint arXiv:2502.13923*, 2025.

[3] Chang Chen, Xiuhong Li, Qianchao Zhu, Jiangfei Duan, Peng Sun, Xingcheng Zhang, and Chao Yang. Centauri: Enabling efficient scheduling for communication-computation overlap in large model training via communication partitioning. In *Proceedings of ASPLOS*, pages 178–191, 2024.

[4] Tianqi Chen, Bing Xu, Chiyuan Zhang, and Carlos Guestrin. Training deep nets with sublinear memory cost. *arXiv preprint arXiv:1604.06174*, 2016.

[5] Paul F Christiano, Jan Leike, Tom Brown, Miljan Martic, Shane Legg, and Dario Amodei. Deep reinforcement learning from human preferences. *Advances in Neural Information Processing Systems*, 2017.

[6] Jeffrey Dean and Sanjay Ghemawat. Mapreduce: simplified data processing on large clusters. *Communications of the ACM*, 51(1):107–113, 2008.

[7] Jiafei Duan, Samson Yu, Hui Li Tan, Hongyuan Zhu, and Cheston Tan. A survey of embodied ai: From simulators to research tasks. *Proceedings of IEEE*, 2022.

[8] Lester Randolph Ford and Delbert Ray Fulkerson. Flows in networks. 2015.

[9] Message Passing Interface Forum. Mpi: A message-passing interface standard. <https://www.mpi-forum.org>, 2025.

[10] Wei Fu, Jiaxuan Gao, Xujie Shen, Chen Zhu, Zhiyu Mei, Chui He, Shusheng Xu, Guo Wei, Jun Mei, Jia-shu Wang, et al. Areal: A large-scale asynchronous reinforcement learning system for language reasoning. *arXiv preprint arXiv:2505.24298*, 2025.

[11] Jian Hu. Reinforce++: A simple and efficient approach for aligning large language models. *arXiv preprint arXiv:2501.03262*, 2025.

[12] Jian Hu, Xibin Wu, Zilin Zhu, Weixun Wang, Dehao Zhang, Yu Cao, et al. Openrlhf: An easy-to-use, scalable and high-performance rlhf framework. *arXiv preprint arXiv:2405.11143*, 2024.

[13] Zixiao Huang, Junhao Hu, Hao Lin, Chunyang Zhu, Yueran Tang, Quanlu Zhang, Zhen Guo, Zhenhua Li, Shengen Yan, Zhenhua Zhu, et al. Reducing gpu memory fragmentation via spatio-temporal planning for efficient large-scale model training. *arXiv preprint arXiv:2507.16274*, 2025.

[14] Michael Isard, Mihai Budiu, Yuan Yu, Andrew Birrell, and Dennis Fetterly. Dryad: distributed data-parallel programs from sequential building blocks. In *Proceedings of EuroSys*, pages 59–72, 2007.

[15] Anand Jayaraman, Jinliang Wei, Garth Gibson, Alexandra Fedorova, and Gennady Pekhimenko. Priority-based parameter propagation for distributed dnn training. *Proceedings of MLSys*, 1:132–145, 2019.

[16] Moo Jin Kim, Chelsea Finn, and Percy Liang. Fine-tuning vision-language-action models: Optimizing speed and success. *arXiv preprint arXiv:2502.19645*, 2025.

[17] Moo Jin Kim, Karl Pertsch, Siddharth Karamcheti, Ted Xiao, Ashwin Balakrishna, Suraj Nair, Rafael Rafailov, Ethan Foster, Grace Lam, Pannag Sanketi, Quan Vuong, Thomas Kollar, Benjamin Burchfiel, Russ Tedrake, Dorsa Sadigh, Sergey Levine, Percy Liang, and Chelsea Finn. Openvla: An open-source vision-language-action model. *arXiv preprint arXiv:2406.09246*, 2024.

[18] Haozhan Li, Yuxin Zuo, Jiale Yu, Yuhao Zhang, Zhao-hui Yang, Kaiyan Zhang, Xuekai Zhu, Yuchen Zhang, Tianxing Chen, Ganqu Cui, Dehui Wang, Dingxiang Luo, Yuchen Fan, Youbang Sun, Jia Zeng, Jiangmiao Pang, Shanghang Zhang, Yu Wang, Yao Mu, Bowen Zhou, and Ning Ding. Simplevla-rl: Scaling vla training via reinforcement learning, 2025.

[19] Shenggui Li, Hongxin Liu, Zhengda Bian, Jiarui Fang, Haichen Huang, Yuliang Liu, Boxiang Wang, and Yang You. Colossal-ai: A unified deep learning system for large-scale parallel training. In *Proceedings of ICPP*, pages 766–775, 2023.

[20] Bo Liu, Yifeng Zhu, Chongkai Gao, Yihao Feng, Qiang Liu, Yuke Zhu, and Peter Stone. Libero: Benchmarking knowledge transfer for lifelong robot learning. *arXiv preprint arXiv:2306.03310*, 2023.

[21] Jijia Liu, Feng Gao, Bingwen Wei, Xinlei Chen, Qingmin Liao, Yi Wu, Chao Yu, and Yu Wang. What can rl bring to vla generalization? an empirical study, 2025.

[22] Kshiteej Mahajan, Ching-Hsiang Chu, Srinivas Sridharan, and Aditya Akella. Better together: Jointly optimizing ml collective scheduling and execution planning using syndicate. In *Proceedings of NSDI*, pages 809–824, 2023.

[23] Chen Meng, Minmin Sun, Jun Yang, Minghui Qiu, and Yang Gu. Training deeper models by gpu memory optimization on tensorflow. In *Proceedings of ML Systems Workshop in NIPS*, volume 7, 2017.

[24] Philipp Moritz, Robert Nishihara, Stephanie Wang, Alexey Tumanov, Richard Liaw, Eric Liang, Melih Elibol, Zongheng Yang, William Paul, Michael I Jordan, et al. Ray: A distributed framework for emerging {AI} applications. In *13th USENIX symposium on operating systems design and implementation (OSDI 18)*, pages 561–577, 2018.

[25] Derek G Murray, Frank McSherry, Rebecca Isaacs, Michael Isard, Paul Barham, and Martín Abadi. Naiad: a timely dataflow system. In *Proceedings of SOSP*, pages 439–455, 2013.

[26] Reiichiro Nakano, Jacob Hilton, Suchir Balaji, Jeff Wu, Long Ouyang, Christina Kim, Christopher Hesse, Shantanu Jain, Vineet Kosaraju, William Saunders, et al. Webgpt: Browser-assisted question-answering with human feedback. *arXiv preprint arXiv:2112.09332*, 2021.

[27] NVIDIA. Nvidia collective communications library (nccl). <https://developer.nvidia.com/nccl>, 2025.

[28] OpenAI. Learning to reason with llms. <https://openai.com/index/learning-to-reason-with-llms/>, 2025.

[29] Long Ouyang, Jeffrey Wu, Xu Jiang, Diogo Almeida, Carroll Wainwright, Pamela Mishkin, Chong Zhang, Sandhini Agarwal, Katarina Slama, Alex Ray, et al. Training language models to follow instructions with human feedback. *Advances in neural information processing systems*, 35:27730–27744, 2022.

[30] PyTorch. Gloo: Collective communications library. <https://github.com/pytorch/gloo>, 2025.

[31] Qwen, :, An Yang, Baosong Yang, Beichen Zhang, Binyuan Hui, Bo Zheng, Bowen Yu, Chengyuan Li, Dayiheng Liu, Fei Huang, Haoran Wei, Huan Lin, Jian Yang, Jianhong Tu, Jianwei Zhang, Jianxin Yang, Jiaxi Yang, Jingren Zhou, Junyang Lin, Kai Dang, Keming Lu, Keqin Bao, Kexin Yang, Le Yu, Mei Li, Mingfeng Xue, Pei Zhang, Qin Zhu, Rui Men, Runji Lin, Tianhao Li, Tianyi Tang, Tingyu Xia, Xingzhang Ren, Xuancheng Ren, Yang Fan, Yang Su, Yichang Zhang, Yu Wan, Yuqiong Liu, Zeyu Cui, Zhenru Zhang, and Zihan Qiu. Qwen2.5 technical report, 2025.

[32] Samyam Rajbhandari, Jeff Rasley, Olatunji Ruwase, and Yuxiong He. Zero: Memory optimizations toward training trillion parameter models. In *Proceedings of SC*, pages 1–16, 2020.

[33] Samyam Rajbhandari, Olatunji Ruwase, Jeff Rasley, Shaden Smith, and Yuxiong He. Zero-infinity: Breaking the gpu memory wall for extreme scale deep learning. In *Proceedings of SC*, pages 1–14, 2021.

[34] Jeff Rasley, Samyam Rajbhandari, Olatunji Ruwase, and Yuxiong He. Deepspeed: System optimizations enable training deep learning models with over 100 billion parameters. In *Proceedings of SIGKDD*, pages 3505–3506, 2020.

[35] Jie Ren, Samyam Rajbhandari, Reza Yazdani Aminabadi, Olatunji Ruwase, Shuangyan Yang, Minjia Zhang, Dong Li, and Yuxiong He. Zero-offload: Democratizing billion-scale model training. In *Proceedings of ATC*, pages 551–564, 2021.

[36] John Schulman, Filip Wolski, Prafulla Dhariwal, Alec Radford, and Oleg Klimov. Proximal policy optimization algorithms. *arXiv preprint arXiv:1707.06347*, 2017.

[37] Zhihong Shao, Peiyi Wang, Qihao Zhu, Runxin Xu, Junxiao Song, Xiao Bi, Haowei Zhang, Mingchuan Zhang, YK Li, Yang Wu, et al. Deepseekmath: Pushing the limits of mathematical reasoning in open language models. *arXiv preprint arXiv:2402.03300*, 2024.

[38] Gerald Shen, Zhilin Wang, Olivier Delalleau, Jiaqi Zeng, Yi Dong, Daniel Egert, Shengyang Sun, Jimmy Zhang, Sahil Jain, Ali Taghibakhshi, et al. Nemo-aligner: Scalable toolkit for efficient model alignment. *arXiv preprint arXiv:2405.01481*, 2024.

[39] Guangming Sheng, Chi Zhang, Zilingfeng Ye, Xibin Wu, Wang Zhang, Ru Zhang, Yanghua Peng, Haibin Lin, and Chuan Wu. Hybridflow: A flexible and efficient rlhf framework. In *Proceedings of the Twentieth European Conference on Computer Systems*, pages 1279–1297, 2025.

[40] Mohammad Shoeybi, Mostofa Patwary, Raul Puri, Patrick LeGresley, Jared Casper, and Bryan Catanzaro. Megatron-lm: Training multi-billion parameter language models using model parallelism. *arXiv preprint arXiv:1909.08053*, 2019.

[41] Stone Tao, Fanbo Xiang, Arth Shukla, Yuzhe Qin, Xander Hinrichsen, Xiaodi Yuan, Chen Bao, Xinsong Lin, Yulin Liu, Tse kai Chan, Yuan Gao, Xuanlin Li, Tongzhou Mu, Nan Xiao, Arnav Gurha, Viswesh Na-gaswamy Rajesh, Yong Woo Choi, Yen-Ru Chen, Zhiao Huang, Roberto Calandra, Rui Chen, Shan Luo, and Hao Su. Maniskill3: Gpu parallelized robotics simulation and rendering for generalizable embodied ai. *Robotics: Science and Systems*, 2025.

[42] Physical Intelligence team. openpi holds open-source models and packages for robotics. <https://github.com/Physical-Intelligence/openpi>, 2025.

[43] Huggingface xDAN-datasets (xDAN Back). xdan-datasets/areal-boba-data. <https://huggingface.co/datasets/xDAN-datasets/AReAL-boba-Data>, 2025.

[44] Zhewei Yao, Reza Yazdani Aminabadi, Olatunji Ruwase, Samyam Rajbhandari, Xiaoxia Wu, Ammar Ahmad Awan, Jeff Rasley, Minjia Zhang, Conglong Li, Connor Holmes, et al. Deepspeed-chat: Easy, fast and affordable rlhf training of chatgpt-like models at all scales. *arXiv preprint arXiv:2308.01320*, 2023.

[45] Qiying Yu, Zheng Zhang, Ruofei Zhu, Yufeng Yuan, Xiaochen Zuo, Yu Yue, Weinan Dai, Tiantian Fan, Gao-hong Liu, Lingjun Liu, et al. Dapo: An open-source llm reinforcement learning system at scale. *arXiv preprint arXiv:2503.14476*, 2025.

[46] Matei Zaharia, Reynold S Xin, Patrick Wendell, Tathagata Das, Michael Armbrust, Ankur Dave, Xiangrui Meng, Josh Rosen, Shivaram Venkataraman, Michael J Franklin, et al. Apache spark: a unified engine for big data processing. *Communications of the ACM*, 59(11):56–65, 2016.

[47] Yanli Zhao, Andrew Gu, Rohan Varma, Liang Luo, Chien-Chin Huang, Min Xu, Less Wright, Hamid Shojanazeri, Myle Ott, Sam Shleifer, et al. Pytorch fsdp: experiences on scaling fully sharded data parallel. *arXiv preprint arXiv:2304.11277*, 2023.

[48] Lianmin Zheng, Zhuohan Li, Hao Zhang, Yonghao Zhuang, Zhifeng Chen, Yanping Huang, Yida Wang, Yuanzhong Xu, Danyang Zhuo, Eric P Xing, et al. Alpa: Automating inter-and {Intra-Operator} parallelism for distributed deep learning. In *Proceedings of OSDI*, pages 559–578, 2022.

[49] Lianmin Zheng, Liangsheng Yin, Zhiqiang Xie, Chuyue Sun, Jeff Huang, Cody Hao Yu, Shiyi Cao, Christos Kozyrakis, Ion Stoica, Joseph E. Gonzalez, Clark Barrett, and Ying Sheng. Sclang: Efficient execution of structured language model programs, 2024.

[50] Yuxiang Zheng, Dayuan Fu, Xiangkun Hu, Xiaojie Cai, Lyumanshan Ye, Pengrui Lu, and Pengfei Liu. Deepresearcher: Scaling deep research via reinforcement learning in real-world environments. *arXiv preprint arXiv:2504.03160*, 2025.